

A Tunable Anomalous Hall Effect in a Non-Ferromagnetic System

J. Cumings^{1,3}, L. S. Moore¹, H. T. Chou², K. C. Ku⁴, G. Xiang⁴, S. A. Crooker⁵, N. Samarth⁴, D. Goldhaber-Gordon¹

Departments of ¹Physics and ²Applied Physics, Stanford University, Stanford, CA 94305; ³Department of Materials Science and Engineering, University of Maryland, College Park, MD 20742; ⁴Department of Physics, Pennsylvania State University, University Park, PA 16802; ⁵National High Magnetic Field Laboratory, Los Alamos, NM 87545

(Dated: October 31, 2018)

We measure the low-field Hall resistivity of a magnetically-doped two-dimensional electron gas as a function of temperature and electrically-gated carrier density. Comparing these results with the carrier density extracted from Shubnikov-de Haas oscillations reveals an excess Hall resistivity that increases with decreasing temperature. This excess Hall resistivity qualitatively tracks the paramagnetic polarization of the sample, in analogy to the ferromagnetic anomalous Hall effect. The data are consistent with skew-scattering of carriers by disorder near the crossover to localization.

PACS numbers: 75.50.Pp, 71.70.Ej, 85.30.Tv

The transverse, or Hall, resistivity is a direct measure of the sign and concentration of charge carriers in most materials. However, other subtler electronic properties can produce “anomalous” corrections to the Hall resistivity. Such anomalous Hall effects (AHE) are well-known for correlated-electron systems such as ferromagnetic metals [1], type-II superconductors [2], weakly-localized conductors [3], and Kondo-lattice materials [4]. Although it has been known for almost as long as the Hall effect itself, the AHE in ferromagnetic materials remains the subject of contemporary debate and has gained renewed interest due to its close theoretical connection to the recently discovered spin-Hall effect and to spin transport in general [5, 6, 7, 8, 9, 10]. Since this AHE often persists above the ferromagnetic Curie temperature, an analogous AHE should be observable in a purely paramagnetic system, in which the charge carriers are spin polarized by an external magnetic field [9]. Unlike ferromagnetic metals whose spin polarization is fixed by their chemistry [11], paramagnetic semiconductors present the additional advantage that their magnetic properties can be smoothly tuned by varying carrier density, magnetic field, or temperature in a given sample. This provides an ideal opportunity to clarify the mechanisms of the AHE. Unfortunately, previous studies in narrow gap semiconductors (e.g. n-InSb) revealed only a very weak AHE, despite large *g*-factors and strong spin-orbit coupling [9], conditions which should favor observing the AHE. Diluted magnetic semiconductors (DMS) have shown a clear AHE, but only in samples that exhibit hole-mediated ferromagnetism [12], with limited opportunity for tuning with an electric field [13]. Bulk crystals of n-type DMS are not ferromagnetic and, despite their extremely large spin splitting, have exhibited no AHE in previous studies [14].

Here, we report the observation of a robust and tunable AHE in a purely paramagnetic two-dimensional electron gas in a DMS quantum well. Surprisingly, the effect is much larger than in earlier studies of paramagnetic

semiconductors, despite the presence of a large bandgap and—hence—a weak spin-orbit coupling. We show that the strength of the AHE is electrically tunable in this system, shedding new light on the origins of this class of phenomena and suggesting the possibility of gate-tunable spin transport in similar structures. Finally, we identify a remarkably simple dependence of our AHE on classical scattering in the regime of localization.

We have chosen to study the AHE in magnetically-doped two-dimensional electron gases (M2DEGs) [15, 16] derived from a II-VI DMS [17]. This choice is dictated by several factors: (a) the carriers have an unusually large paramagnetic susceptibility, resulting in a significant spin polarization that enhances the strength of the AHE; (b) the 2D nature and moderately high mobility (due to modulation doping) allow independent measurement of the carrier density through Shubnikov-de Haas (SdH) oscillations; (c) the paramagnetic susceptibility can be tuned by varying the temperature; (d) at a fixed temperature, other properties such as the carrier density, Fermi energy and resistivity are tunable using the electric field from a gate electrode on the sample surface.

The samples consist of a modulation-doped single quantum well (10.5 nm thickness) of $Zn_{1-x-y}Cd_yMn_xSe$ ($x \sim 0.02$, $y \sim 0.12$) sandwiched between ZnSe barriers. Symmetrically placed n-type ZnSe layers (25 nm thick), spaced 12.5 nm from the quantum well by intrinsic ZnSe spacer layers, donate free electrons to the well. The material is described in more detail elsewhere [15, 16]. The Mn ions behave essentially as free spin-5/2 moments with Brillouin-like paramagnetic susceptibility. Polarization of the Mn induces a spin-splitting in the conduction electrons through an *s* – *d* exchange coupling, giving the carriers an effective *g*-factor far higher than even small-bandgap semiconductors: $g \sim 80$ in our material at 1.5 K, producing complete polarization of carriers at ~ 1 T. The structures were patterned into 100 μ m wide Hall bars by photolithography and wet-etching, and annealed indium metal provided ohmic contact to the buried 2DEG. In

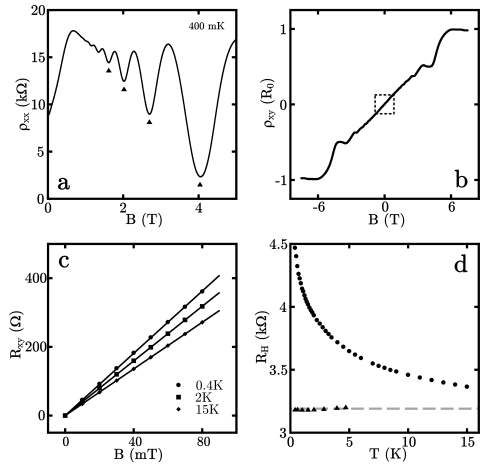


FIG. 1: a) & b) The longitudinal and Hall resistances of a M2DEG, revealing SdH oscillations and quantum Hall plateaus. The small box in (b) schematically indicates the low-field region of (c) ($R_0 = 12.9\text{k}\Omega$). c) The Hall resistance at a variety of temperatures. d) R_H as a function of temperature. The density indicated by the arrows in (a) would be expected to give an R_H of 3190\Omega/Tesla , as indicated by the dashed line in (c). The triangles show the results of similar SdH measurements performed over a range of temperatures.

some samples, a gate electrode (10 nm Ti/100 nm Au) was deposited by electron-beam evaporation. Transverse and longitudinal resistances were measured in a ^3He cryostat with a base temperature of 290 mK using a 5 Hz lock-in technique at 30 nA RMS excitation current [18].

In Figs.1 (a) and 1(b), we show the magnetic field dependence of the longitudinal and transverse resistance, respectively, for a sample at $T = 0.4\text{ K}$, revealing SdH oscillations and an integer quantum Hall effect at high fields. The arrows marking the minima in Fig. 1(a) correspond to the (spin-resolved) $\nu=2, 3, 4$, and 5 Landau levels, consistent with a sheet density $n_s = 1.96 \times 10^{11}\text{ cm}^{-2}$ which does not vary over the temperature range $0.4\text{ K} < T < 2\text{ K}$. In Fig. 1(c), we show the field-dependence of the Hall resistance (R_{Hall}) at low fields. In this regime, R_{Hall} is linear in B , with a slope usually identified as the ordinary Hall coefficient, $R_H = (n_s e)^{-1}$ [19]. However, R_H clearly changes significantly between 0.4 K and 15 K, even though there is no accompanying change in n_s as determined from SdH data. Figure 1(d) compares the temperature variation of R_H with that of the ordinary value calculated using n_s : clearly, R_H is anomalously high at low temperatures, gradually approaching its ordinary value at higher temperatures. As we show later, the temperature-dependence of R_H closely follows that of the paramagnetic susceptibility of the magnetic ions. Similar behavior is found upon a re-examination of low field Hall data from measurements in other M2DEG samples [16], suggesting that the phenomenon is generic to this system.

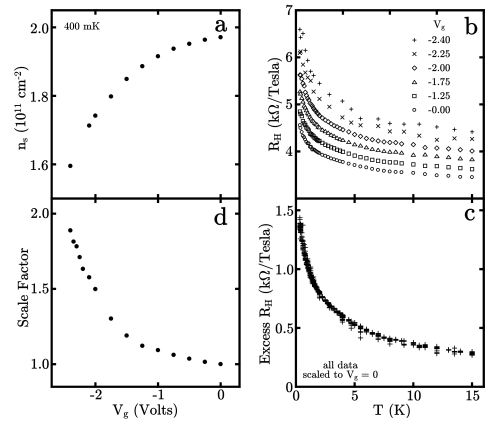


FIG. 2: The gate-voltage dependence of sample characteristics. a) Variation of carrier density (as determined from SdH oscillations). b) R_H at various values of T and V_g . c) All the data sets from (b) can be collapsed onto a single curve, by subtracting the ordinary Hall coefficient for the density measured in (a) and dividing by a scale factor. d) The resulting scale factors.

To tune the AHE, we fabricated a large-area gate electrode on a second Hall bar from the same heterostructure. Measurements of SdH oscillations show that the application of a negative gate voltage (V_g) decreases n_s (Fig. 2(a)) as expected. Application of a negative gate voltage also affects the measured value of R_H (Fig. 2(b)). Consistent with a decrease in n_s , we find an increase in R_H . In addition, R_H becomes more strongly temperature-dependent, indicating an increase in the strength of the AHE. To extract the AHE strength, we collapse all the data onto the same curve by first subtracting the calculated value of the ordinary Hall coefficient and then dividing by a V_g -dependent scale factor (deduced from a least-squares fit). Figure 2(c) shows that this procedure collapses all data sets onto the same characteristic T-dependence. Figure 2(d) shows the extracted scale factors, normalized to unity at $V_g = 0$, demonstrating that the strength of the AHE can be electrically tuned by nearly a factor of two.

The empirical form for the AHE is given by

$$R_{xy} = 1/(en_s)B + R_s M. \quad (1)$$

where the first term is the ordinary Hall resistance, proportional to magnetic field B and inversely proportional to the charge per carrier (e) and the sheet density of carriers (n_s). The second term is the anomalous contribution, proportional to the magnetic moment M of the system. In the M2DEG studied here, M is the spin-polarization of the carriers, which is in turn proportional to the magnetization of the local Mn moments at low fields. The magnetization of the paramagnetic local Mn moments is empirically known to follow a modified Curie-Weiss law, $M \sim B/(T+T_0)$, in the low field limit where T_0 is a phenomenological parameter that accounts for the short-

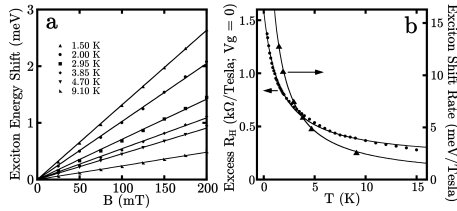


FIG. 3: Results of photoluminescence studies. a) The exciton shift as a function of B for a variety of temperatures. This shift is proportional to electronic magnetization. b) The low-field linear coefficient of the exciton shift, superimposed on the low-field excess R_H (at $V_g = 0$). The lines represent least-squares fits as described in the text.

range coupling of neighboring Mn spins [17]. Eq. (1) thus predicts that R_{xy} is linear in B , and the AHE must be separated from the ordinary temperature-independent Hall effect by examining the T dependence of R_H .

The AHE is commonly characterized by measuring M and extracting the constant of proportionality R_s from Eq. (1). In our sample, M is too small to measure by conventional susceptometry methods and micro-fabricated cantilever measurements require specially-designed heterostructures [20]. Hence, we extract M from the enhanced Zeeman shift of spin-sensitive photoluminescence (PL) [21]. In these measurements, photo-excited electrons and holes form excitons, which then decay radiatively. The large Zeeman-shift of the PL peak is directly proportional to the Zeeman-splitting and the relative magnetization of the electrons in the conduction band, which accurately tracks the Brillouin-like magnetization of the paramagnetic Mn local moments in the M2DEG [17]. To closely match the results of the different measurements, neighboring pieces of the same sample were used for PL and transport.

In Fig. 3(a), we show results of the PL measurements, with fits to a spin-5/2 Brillouin function, including weak antiferromagnetic coupling characterized by T_0 [17]. These fits yield T_0 ranging from 0.69 K to 1.03 K, in agreement with previous studies of similar M2DEGs. In Fig. 3(b), we compare the low-field behavior of the PL shift with that of the AHE by plotting the T -dependence of both the linear coefficient of the PL shift and the excess R_H (at $V_g = 0$). The PL shift rate is fit to a Curie-Weiss law [$C/(T+T_0)$] and R_H is fit to [$A+C/(T+T_0)$]. These fits yield $T_0^{\text{PL}} = 0.53$ and $T_0^{\text{Hall}} = 1.58$. The A parameter of the R_H fit gives $n_s = 1.87 \times 10^{11} \text{ cm}^{-2}$ in good agreement with the SdH-determined value of $1.96 \times 10^{11} \text{ cm}^{-2}$ [22]. This agreement demonstrates that the excess R_H observed in these samples scales directly with the sample magnetization and therefore shares common origins with the AHE of ferromagnetic systems [23].

We now turn to a discussion of theoretical models of

the AHE and their relation to our system. We note at the outset that the spin-orbit (SO) coupling in our system is relatively weak, characterized by a parameter λ more than 10 times smaller than for GaAs and more than 1000 times smaller than for InSb. Weak SO coupling is confirmed by the absence of weak antilocalization in low field magnetoresistance measurements of non-magnetic versions of our host material [15]. This low SO coupling demands that we look in detail at the origin of the observed AHE. Our material could exhibit an AHE of intrinsic origin (unrelated to disorder potentials) if there were an electric field perpendicular to the 2DEG strong enough to induce a Rashba SO splitting [10]. However, our quantum well is designed to be symmetric, without any electric field. As an extreme case, if we assume a completely asymmetric well, with the sheet density entirely compensated by an electric field on one side, the strength of this field would be $4 \times 10^6 \text{ V/m}$. Even in this limit—and with all other assumptions as generous as possible—the intrinsic effect could account for only 6% of the observed deviation (at $V_g = 0$, $T = 1\text{K}$) [10]. Another potential source of intrinsic AHE is the strain-induced SO splitting due to lattice mismatch at the growth interface. However, the leading contribution is from off-diagonal strain due to shear stress, and a simple calculation shows even this effect to be negligible. Therefore, intrinsic effects are insufficient to account for our AHE, which must instead be caused by disorder-induced scattering. A simple theory incorporating both skew-scattering and sidejump-scattering predicts an excess Hall resistivity:

$$\Delta\rho_{xy} = 2\pi V m^* \lambda \langle \mu_z \rangle n_s \rho_{xx} + 2e^2 \lambda \langle \mu_z \rangle n_s \rho_{xx}^2, \quad (2)$$

where λ is a measure of the strength of the SO coupling in the material; V is the potential of individual δ -function scatterers, which can be either positive (repulsive) or negative (attractive); $\langle \mu_z \rangle$ is the averaged spin magnetic moment per carrier (in units of Bohr magnetons); and ρ_{xx} , m^* , and e are the longitudinal resistivity, effective mass, and charge per carrier, respectively [24, 25]. The first and second terms originate from skew scattering and sidejump scattering, respectively. In the II-VI quantum wells studied here, λ is known to be negative, as the g -factor for electrons in the conduction band is reduced relative to its vacuum value due to spin-orbit coupling in the semiconductor [26]. The sidejump term hence has a sign opposite to that of the ordinary Hall effect and cannot account for our observations. Further, the strength of the sidejump term predicted by Eq. (2) only amounts to about 1% of the observed AHE (at $V_g = 0$, $T = 1\text{K}$) [25]. Having exhausted other options, we tentatively link our positive AHE to skew scattering from scatterers with attractive potentials (V negative). This would be confirmed by observing a clear linear dependence of the AHE on ρ_{xx} .

Figure 4(a) shows ρ_{xx} as a function of both V_g and T .

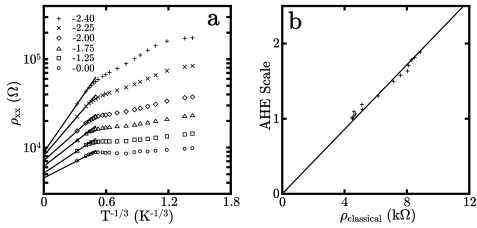


FIG. 4: The dependence of the AHE on sample resistivity. a) Longitudinal resistivity is plotted against $T^{-1/3}$ for a variety of V_g values. The lines are extrapolations to $T \rightarrow \infty$ from the two highest temperature points. b) The strength of the AHE (as measured by the scale factor in Fig. 2(d)) is plotted against the classical resistivity (as described in the text). The line represents a single-parameter fit to the data using a linear form with no constant term.

At the lowest temperatures, ρ_{xx} varies by about a factor of twenty as a function of V_g . Within the same V_g range, the strength of the AHE (Fig. 2(d)) varies by only a factor of two, clearly demonstrating a weaker-than-linear dependence on ρ_{xx} . We are unaware of any previous theoretical prediction of such weak ρ_{xx} -dependence for an AHE, and we suggest localization as a plausible explanation. In our sample, as the strength of the gate voltage is increased ρ_{xx} passes through the quantum of resistance, ~ 12.9 kΩ, at about $V_g = -1.5$ V and increases rapidly at low T , indicative of localization. To account for this, we suggest the ansatz $\rho_{xx}(T) = \rho_{classical} + \rho_{localization}(T)$, and propose that $\rho_{classical}$ replaces ρ_{xx} in Eq. 2 for this regime. To extract $\rho_{classical}$ from our data, we use the theory of two-dimensional variable range hopping (2DVRH), which predicts [27]

$$\rho_{xx}(T) = \rho_0 \exp[(T_{VRH}/T)^{1/3}] \quad (3)$$

This form yields an easily extractable high-temperature limit, ρ_0 . To test if this is the correct form, in Fig. 4(a) we plot ρ_{xx} vs. $T^{-1/3}$ on a log scale which should give straight lines for 2DVRH. The data are not strictly linear, probably because they are taken at the onset of localization and not in the regime of strong localization. Nevertheless, extrapolating the data from the two highest temperature points yields ρ_0 values that we use as estimates for $\rho_{classical}$. Figure 4(b) shows the AHE scale factors from Fig. 2(d) plotted as a function of $\rho_{classical}$, in comparison with Eq. (2) [28]. A linear fit through the data extrapolates to the origin (with no offset), demonstrating that the AHE strength scales linearly with the Drude/Boltzmann classical resistance and offering further evidence for the skew-scattering origin of the AHE. If we use Eq. (2) and the slope from Fig. 4(b), and we take the size of the skew scattering sites to be λ_F^2 , we extract a scattering potential V on the order of -20 meV, which is plausible for this ~ 2.5 eV gap semiconductor.

In summary, we have reported the surprising observation of a robust AHE in a non-ferromagnetic 2DEG, de-

spite a very weak SO coupling. Electrical gating allows us to study the AHE as a function of carrier density, and—hence—disorder. Our data are consistent with an AHE that originates in impurity-related skew scattering, but we find clear deviations from standard theoretical expectations with increasing disorder, particularly beyond the crossover to localization [29]. These results suggest the possible emergence of new physics from the interplay between disorder and the AHE, which we hope will motivate the development of new theories that address this issue. We finally note that, while the AHE produces an excess Hall resistance in our M2DEG at low field, the quantum Hall effect plateaus remain properly quantized at high field. This raises interesting questions about the interplay between the two phenomena.

The authors thank A. H. MacDonald for initially suggesting the measurements and B. A. Bernevig for extensive discussions. The work at Stanford was supported by the ONR under contracts N00014-02-1-0986 and N00014-01-1-0569(YIP), and was performed in part at the Stanford Nanofabrication Facility of NNIN supported by the National Science Foundation under Grant ECS-9731293. Work at PSU was supported by ONR under contract N00014-02-1-0996.

- [1] C. M. Hurd, *The Hall Effect in Metals and Alloys* (Plenum, New York, 1973), Ch. 5; G. Bergmann, Physics Today **32**, 25 (1979); J. Sinova, T. Jungwirth, and J. Cerne, Int. J. Mod. Phys. B **18**, 1083 (2004), §3.4.
- [2] S. J. Hagen *et al.*, Phys. Rev. B **43**, R6246 (1991).
- [3] V. J. Goldman *et al.*, Phys. Rev. Lett. **57**, 1056 (1986); M. Sawicki and T. Dietl, in *Proceedings of the 19th International Conference on the Physics of Semiconductors*, edited by W. Zawadzki, (Institute of Physics, Polish Academy of Sciences, Warsaw, 1988) p. 1217.
- [4] N. B. Brandt and V. V. Moshchalkov, Adv. Phys. **33**, 373 (1984).
- [5] M. I. D'yakonov, V. I. Perel, JETP Lett. **13**, 467 (1971); M. I. D'yakonov, V. I. Perel, Phys. Lett. A **35**, 459 (1971).
- [6] J. E. Hirsch, Phys. Rev. Lett. **83**, 1834 (1999).
- [7] S. Zhang, Phys. Rev. Lett. **85**, 393 (2000).
- [8] Y. K. Kato *et al.*, Science **306**, 1910 (2005); J. Wunderlich *et al.*, Phys. Rev. Lett. **94**, 047204 (2005).
- [9] J.-N. Chazalviel, Phys. Rev. B **11**, 3918 (1975).
- [10] D. Culcer, A. MacDonald, Q. Niu, Phys. Rev. B **68**, 045327 (2003).
- [11] W.-L. Lee *et al.*, Science **303**, 1647 (2004).
- [12] H. Ohno *et al.*, Phys. Rev. Lett. **68**, 2664 (1992); H. Ohno, Science **281**, 951 (1998); D. Ferrand *et al.*, Phys. Rev. B **63**, 085201 (2001).
- [13] H. Ohno *et al.*, Nature **408**, 944 (2000).
- [14] Y. Shapira *et al.*, Phys. Rev. B **41**, 5931 (1990).
- [15] I. P. Smorchkova *et al.*, Phys. Rev. Lett. **78**, 3571 (1997); I. P. Smorchkova *et al.*, J. Appl. Phys. **81**, 4858 (1997).
- [16] R. Knobel *et al.*, Physica E **6**, 786 (2000); R. Knobel *et al.*, Phys. Rev. B **65**, 235327 (2002).

[17] J. K. Furdyna, *J. Appl. Phys.* **64**, R29 (1988).

[18] Measured resistance values show no significant change when the current is lowered to 10 nA. Measurements at 150 nA show subtle differences attributable to electron heating. The AC lock-in frequency of 5 Hz was chosen to maximize measurement speed. A phase lag in the sample's response introduces a small systematic error in our measurement of the Hall resistance. This error is 0.1% at 5 Hz, and increases with increasing frequency. As observed previously in similar samples, the capacitance responsible for the phase lag is associated with the heterostructure, not the measurement setup.

[19] R_H is determined by fitting the R_{xy} data to a linear form in the range of $90 \text{ mT} < B < 90 \text{ mT}$. For some pairs of sample contacts, a strong capacitive signal of unknown origin is observed below the critical field of the superconducting indium contacts ($H_c \sim 25 \text{ mT}$). In these cases, the fitting is confined to the range $30 \text{ mT} < |B| < 90 \text{ mT}$. Polynomial fits were also attempted up to cubic or quintic terms, without significant change to the extracted R_H values. Analyzing the Hall conductivity, σ_{xy} , instead of R_{xy} results in no change to the interpretation of the AHE.

[20] J. G. E. Harris *et al.*, *Phys. Rev. Lett.* **86**, 4644 (2001).

[21] Photoluminescence measurements carried out at $10\times$ lower power gave similar results, ruling out bulk heating or similar non-equilibrium effects.

[22] Fixing the A parameter to exactly match the SdH density gives a noticeably worse fit and a $T_0^{\text{Hall}} = 2.93$. T_0 is a phenomenological parameter that depends sensitively on the details of the fit; the difference between $T_0^{\text{PL}} = 0.53$ and $T_0^{\text{Hall}} = 1.58$ is not alarming.

[23] Recent 2D screening models of the temperature-dependence of Hall resistance [S. Das Sarma and E. H. Hwang, *Phys. Rev. Lett.* **95**, 016401 (2005)] cannot alone explain our data, as the related parameter in our system ($qTF/2k_F \sim 3$) is not in the regime of low-T R_{Hall} enhancement [X. P. A. Gao *et al.*, *Phys. Rev. Lett.* **93**, 256402 (2005)], but R_{Hall} suppression [A. Y. Kuntsevich *et al.*, *JETP Lett.* **81**, 409 (2005)].

[24] B. A. Bernevig, private communication.

[25] P. Nozieres and C. Lewiner, *J. Phys.* **34**, 901 (1973).

[26] M. Willatzen, M. Cardona, and N. E. Christensen, *Phys. Rev. B* **51**, 17992 (1995).

[27] W. Brenig, G. H. Döhler, and H. Heyszenau, *Phil. Mag.* **27**, 1093 (1973).

[28] The leading gate-voltage dependence of $\Delta\rho_{xy}$ from the first term of Eq. (2) is ρ_{xx} . The mean carrier magnetic moment $\langle\mu_z\rangle$ is proportional to n_s^{-1} in a simple Fermi gas model, and the quantity $\langle\mu_z\rangle n_s$ therefore has no dependence on density or gate-voltage. All other parameters are expected to be constant.

[29] A. A. Burkov and L. Balents, *Phys. Rev. Lett.* **91**, 057202 (2003).